

## Theoretical Study on the Mechanism of Catalysis of Coenzyme B<sub>12</sub>-Dependent Diol Dehydratase

Masataka Eda, Takashi Kamachi,<sup>#</sup> Kazunari Yoshizawa,<sup>\*,†</sup> and Tetsuo Toraya<sup>\*,††</sup>

Department of Molecular Engineering, Kyoto University, Kyoto 606-8501

<sup>†</sup>Institute for Fundamental Research of Organic Chemistry, Kyushu University, Fukuoka 812-8581

<sup>††</sup>Department of Bioscience and Biotechnology, Okayama University, Okayama 700-8530

(Received July 27, 2001)

The energy profile of the diol dehydratase reaction is discussed from theoretical calculations at the B3LYP/6-311G\* level of density functional theory. The differences between the energy diagrams of models with and without K<sup>+</sup> ion are rather small except for the substrate binding and the OH group migration. The most important role of K<sup>+</sup> ion in the diol dehydratase catalysis is to fix substrates and intermediates in proper positions in order to ensure the hydrogen abstraction and recombination between them and the adenosyl group. In the course of the reaction, substrates and reaction intermediates would always be kept bound to K<sup>+</sup> ion until the release of product aldehyde from the active site. Given the neutral radical state of the substrate, the OH group migration proceeds in a concerted mechanism. In this process, K<sup>+</sup> ion can work as an inhibitor of intramolecular hydrogen bond, which decreases the activation energy by 4.0 kcal/mol, due to the destabilization of reactant 1,2-dihydroxypropyl radical. The lowering of the activation energy by K<sup>+</sup> ion, however, is rather small, and thus the contributions of active-site amino acid residues to the OH group migration must be taken into consideration to explain that the hydrogen abstraction is the rate-determining step for the overall reaction.

Coenzyme B<sub>12</sub> (AdoCbl), including a Co–C covalent bond in it, is one of the most notable compounds in enzyme chemistry. It is an obligatory cofactor and functions as a reversible radical carrier in several enzymatic reactions. AdoCbl-dependent reactions<sup>1,2</sup> involve carbon skeleton rearrangements, heteroatom eliminations, and intramolecular amino group migrations. These reactions lead to the migration of a hydrogen atom from one carbon atom of substrate to an adjacent carbon atom in exchange for group X, as indicated in Chart 1.



Chart 1.

Enzyme-catalyzed dehydration is an important biochemical reaction. Diol dehydratase,<sup>2</sup> an AdoCbl-dependent enzyme, catalyzes the dehydration of 1,2-diols to the corresponding aldehydes. Extensive studies have been reported since the discovery of this enzyme about forty years ago.<sup>3</sup> Labeling experiments revealed that the OH group migrates from the C-2 to C-1 atom in the reaction.<sup>4,5</sup> In order to catalyze this chemically difficult reaction under neutral or weakly alkaline conditions,<sup>2b,6</sup> one requires AdoCbl as a radical source. Co<sup>II</sup> of cob(II)alamin and an organic radical formed during catalysis

were observed by electron spin resonance (ESR).<sup>7</sup> Large kinetic isotope effects (KIE)<sup>8–10</sup> of  $k_H/k_D = 10\text{--}13$  indicate the involvement of hydrogen atom transfer in the rate-determining step. These experimental results established that this catalytic reaction proceeds by a radical mechanism. As illustrated in the minimal mechanism<sup>2</sup> indicated in Fig. 1, the first step of this enzymatic reaction is triggered by the homolytic cleavage of the Co–C bond in AdoCbl (A in Fig. 1). This organometallic bond is activated when the coenzyme is bound to apoprotein and cleaved upon addition of substrates.<sup>2b,11</sup> Generated 5'-deoxyadenosyl (AdoCH<sub>2</sub>) radical abstracts a hydrogen atom on the C-1 atom of substrate. A subsequent hydroxy group migration affords 1,1-diol radical (2,2-dihydroxy-1-methylethyl radical, product-derived radical) from 1,2-diol radical (1,2-dihydroxypropyl radical, substrate-derived radical) and, after a few steps including recombination with a hydrogen atom from 5'-deoxyadenosine (AdoCH<sub>3</sub>) with a net inversion of configuration at the C-2 atom (propanediol substrate),<sup>11,12</sup> it decomposes into aldehyde and water (B in Fig. 1). This catalytic reaction is irreversible,<sup>13a</sup> and both enantiomers of 1,2-propanediol,<sup>13</sup> 3-fluoro-1,2-propanediol,<sup>8</sup> and ethanediol<sup>9</sup> serve as good substrates. Other diols are less reactive by far,<sup>2c,e,g,14</sup> and some of them are competitive inhibitors or inactivators. It is interesting that glycerol can act as both a good substrate and a potent inactivator.<sup>14b,15</sup>

Some B<sub>12</sub> enzymes including diol dehydratase require monovalent cations<sup>2b,13a,16</sup> (K<sup>+</sup> ion or others with similar ionic radii) for catalytic activity. The requirement of apoenzyme for K<sup>+</sup> ion in the tight binding of AdoCbl has been established.<sup>17</sup> The most striking feature in the crystal structure of diol dehy-

<sup>#</sup> Institute for Fundamental Research of Organic Chemistry, Kyushu University

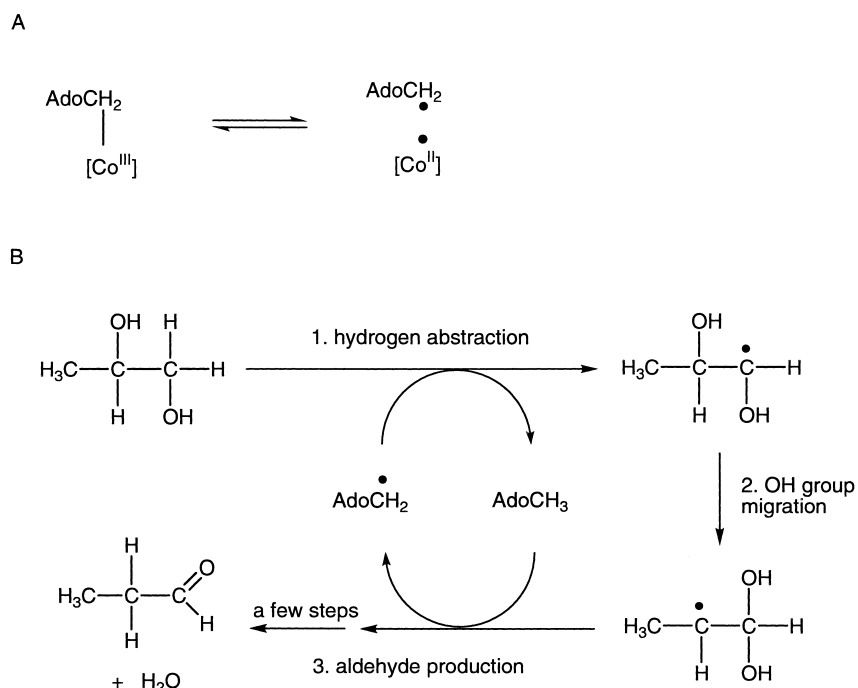


Fig. 1. The minimal mechanism of diol dehydratase reaction. A: Homolytic cleavage of the Co–C bond in AdoCbl. B: AdoCH<sub>2</sub> radical-catalyzed enzymatic dehydration.

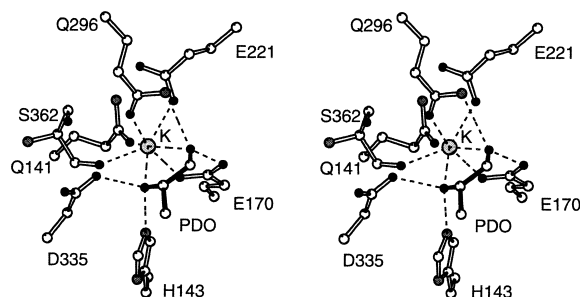


Fig. 2. A stereoview of the active-site residues interacting with the substrate and K<sup>+</sup> ion.<sup>18a</sup> Carbon atoms, oxygen atoms, and nitrogen atoms are shown as open, closed, and meshed circles, respectively. Bonds in the enzyme and substrate are shown as open and closed sticks, respectively.

dehydratase reported recently<sup>18</sup> is that both hydroxy groups of substrate coordinate directly to a K<sup>+</sup> ion that is located in the inner part of the active-site cavity, as shown in Fig. 2. This novel structure implies a direct participation of K<sup>+</sup> ion in the enzymatic reaction. In addition to the striking features mentioned above, the distances between the Co atom in cobalamin and the C-1 and C-2 atoms of substrate in the crystal structure are 8.37 Å and 9.03 Å, respectively. It was proposed by a model study that the C-5'-centered radical of the adenosyl group becomes accessible to the *pro-S* hydrogen atom on C-1 of the substrate by rotation of the ribose moiety around the glycosidic linkage after the Co–C bond cleavage.<sup>18b</sup> These proposals exclude the previous hypothesis<sup>9,19</sup> that Co<sup>II</sup> ion in cobalamin is directly involved in the reaction. Therefore it is highly possible that the reaction proceeds with substrates and intermediates that directly coordinate to K<sup>+</sup> ion.

Before the OH group migration, three types of partially ion-

ic states of substrate are formally considered to occur in the course of the reaction; that is, radical cation arising from partial protonation by amino acid residue(s), neutral radical, and radical anion arising from deprotonation. Although fully protonated radical (radical cation) is unlikely to be involved,<sup>20</sup> possible involvement of partially cationic radical species has been well-documented from ab initio computations by Smith et al.<sup>21</sup> Model studies showed that  $\alpha$ -hydroxy radicals are up to 10<sup>5</sup> times more acidic than corresponding alcohols and rapidly decompose into water and aldehyde radical (1-formylethyl radical) by  $\beta$ -OH cleavage.<sup>22</sup> A stepwise pathway involving a radical anion and a ketyl radical has been described by Bothe et al.<sup>1j</sup> Partially anionic radical species is also possible owing to the existence of Glu<sub>170</sub> being a temporary proton acceptor and the acidity and fragmentation character of  $\alpha$ -hydroxy radical.<sup>18a,23</sup>

Certain enzymes utilize the high reactivity of free radicals to catalyze the reactions.<sup>6</sup> We defined enzymatic radical catalysis as a mechanism of catalysis by which enzymes catalyze chemically difficult reactions utilizing the high reactivity of radicals.<sup>2h</sup> To provide energetic feasibility of the proposed concept of enzymatic radical catalysis,<sup>2h</sup> we present the entire profile of the diol dehydratase reaction from density-functional-theory (DFT) calculations in this work. On the basis of the crystal structure<sup>18</sup> as well as the experimental results,<sup>2</sup> some conceivable intermediates containing K<sup>+</sup> ion and the energetics along the reaction path were computed. Our theoretical analyses gave reaction energy profiles including unstable intermediates for a deeper understanding of the reactions catalyzed by this and other B<sub>12</sub>-dependent enzymes. We have previously shown direct participation of K<sup>+</sup> ion in the catalysis from DFT calculations.<sup>24</sup> No report on a theoretical approach to the whole reaction of diol dehydratase has been made, although the mecha-

nism of the OH group migration has been theoretically studied in detail.<sup>19–21,23–27</sup>

### Computational Details

We computed several possible paths of the diol dehydratase reaction using the hybrid Hartree–Fock/density-functional-theory B3LYP method implemented with the Gaussian 94 ab initio program package.<sup>28</sup> This method consists of the Slater exchange, the Hartree–Fock exchange, the exchange functional of Becke,<sup>29</sup> the correlation functional of Lee, Yang, and Parr (LYP),<sup>30</sup> and the correlation functional of Vosko, Wilk, and Nusair.<sup>31</sup> The triple-zeta 6-311G\* basis set of Pople and co-workers<sup>32</sup> was used for C, O, and H, and the primitive set of Wachters<sup>33</sup> was used for K.<sup>34</sup> We performed structure optimizations on local minima and saddle points (transition state; TS) with models including substrate 1,2-propanediol (or reaction intermediates) and  $K^+$  ion. A vibrational analysis was carried out on each optimized structure to ensure that the structure corresponds to a local minimum that has no imaginary frequency or a saddle point that has only one imaginary frequency. Zero-point vibrational energies were taken into account in calculating the reaction energy profile. On each step of the reaction, some possible isomers (diastereomers) were calculated. Ethyl group was employed as a model of adenosyl group. To better understand the role of  $K^+$  ion in the catalytic function of this  $B_{12}$  enzyme, a model system without  $K^+$  ion was also calculated at the same level of theory. The reaction was considered to proceed via a radical intermediate of substrate. Electrostatic effects of  $K^+$  ion to such a radical species would be weak and therefore the amino acids coordinating to  $K^+$  ion in the crystal structure were ruled out from the models with  $K^+$  ion. The present calculations would overestimate this effect, but a comparison of the systems with  $K^+$  ion and without  $K^+$  ion enables us to judge whether this ligand exclusion entails a large loss of

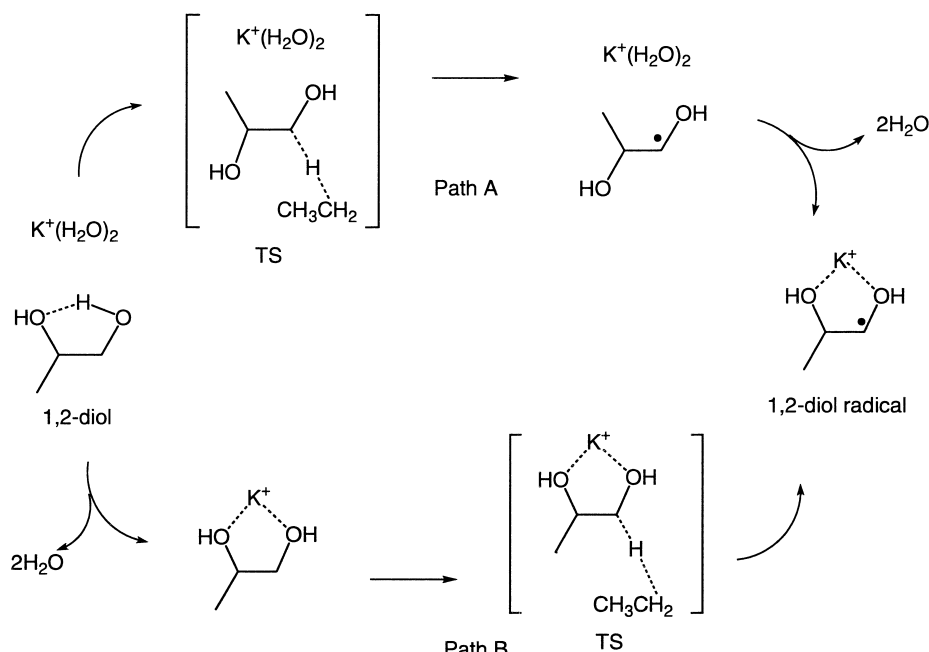
accuracy in the energetics or not.

### Results and Discussion

We partitioned the whole reaction into three electronic processes, as shown in Fig. 1; hydrogen abstraction, OH group migration, and aldehyde production. For the purpose of discussion, the C-1, C-2, C-3, and O atoms of propanediol were designated simply as  $C_{(1)}$ ,  $C_{(2)}$ ,  $C_{(3)}$ ,  $O_{(1)}$ , and  $O_{(2)}$ , respectively. First, we optimized the structure of  $AdoCH_2$  radical and compared its spin density on the C-5 atom with that on the C-1 atom of ethyl radical. We confirmed that ethyl radical is suitable as a model of  $AdoCH_2$  radical except for the steric hindrance of  $AdoCH_2$  radical.

**1. Hydrogen Abstraction:** Crystal structure analyses<sup>18</sup> demonstrated that 1,2-propanediol coordinates to  $K^+$  ion at least before the OH group migrates from  $C_{(2)}$  to  $C_{(1)}$  of substrate radical. Therefore we considered the following two reaction paths for  $K^+$ -1,2-dihydroxypropyl radical complex, as indicated in Scheme 1. In Path A a hydrogen atom on  $C_{(1)}$  of substrate is abstracted by  $AdoCH_2$  radical, which is replaced by ethyl radical in our model, resulting in the formation of 1,2-dihydroxypropyl radical, and the generated radical species is then bound to  $K^+$  ion. In Path B, complexation of substrate with  $K^+$  ion occurs prior to the hydrogen abstraction, which is in the reverse order of Path A.

$K^+$  ion in the crystal structure is seven-coordinated by five oxygen atoms from amino acid residues and two oxygen atoms of hydroxy groups of substrate, as shown in Fig. 2. This is in line with the general trend of  $K^+$  ion since  $K^+$  ion is generally known to be six- to eight coordinated in living organisms.<sup>35</sup> According to the recently determined X-ray structure,<sup>36</sup>  $K^+$  ion in the substrate-free enzyme is also seven-coordinated by five amino acid oxygen atoms and two oxygen atoms from two water molecules in the absence of substrate. The addition of sub-



Scheme 1.

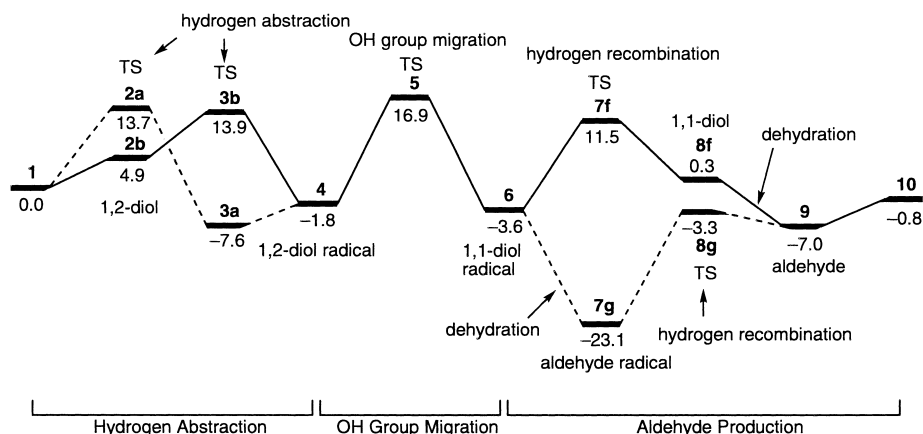


Fig. 3. Energy diagrams of the models with  $K^+$  ion along the reaction path, from 1,2-propanediol to propionaldehyde + water. Hydrogen abstraction process: **1–4** (Path A: dotted lines and Path B: solid lines). OH group migration process: **4–6** (Path E). Aldehyde production process: **6–10** (Path F: solid lines and Path G: dotted lines). The path from **9** to **10** is displacement of product aldehyde from  $K^+$  ion by water. Relative energies are in kcal/mol. Diol and aldehyde denote propanediol and propionaldehyde, respectively.

strate brings about a ligand exchange on  $K^+$  ion and triggers a subsequent conformational change of the protein, which leads the reaction to the next step. The energy of **1** ( $K^+(OH_2)_2^{37} + \text{ethyl radical} + 1,2\text{-propanediol}$  at left in Fig. 3) was taken as a standard (0.0 kcal/mol) to measure the relative energies in the following discussion and in Fig. 3.

Figure 4 shows optimized structures in the first electronic process, “hydrogen abstraction”. Path A starts from  $K^+(OH_2)_2$  and 1,2-propanediol **1** involving an intramolecular hydrogen bond, the energetically most stable geometry among some diastereomers. The activation energy for the hydrogen abstraction (from **1** to **2a** in Fig. 3) was calculated to be 13.7 kcal/mol. We found a lower transition state **2a'** that is directly connected to **1** in a conformational point of view. However, we employed structure **2a** that involves no hydrogen bond because **2a'** is only 1.0 kcal/mol lower in energy and three-point attachment (two OH groups and a methyl group) of substrate to the protein environment was proposed for substrate binding.<sup>10–12</sup> Coordination of the generated substrate radical to  $K^+$  ion brings about energy destabilization with a net binding energy of  $-5.8$  kcal/mol (from **3a** to **4**), accompanying  $(H_2O)_2$  release from  $K^+$  ion. If the generated radical species is temporarily free from protein in the enzyme until binding to  $K^+$  ion, **3a** would be the most stable with respect to the  $C_{(1)}-C_{(2)}$  rotation among the structures without intramolecular hydrogen bond. However, it is likely to form an intramolecular hydrogen bond, and hydrogen-bonded **3a'** is the most stable form with respect to the  $C_{(1)}-C_{(2)}$  rotation, **3a'** lying 4.0 kcal/mol below **3a**, as seen in Fig. 3. In Path B substrate replaces the  $K^+$  ion-bound  $(H_2O)_2$  to form a complex with a net binding energy of  $-4.9$  kcal/mol (from **1** to **2b**) in the initial stage of the reaction. After the complexation, the *pro-S* hydrogen abstraction from (*S*)-1,2-propanediol requires an activation energy of 9.0 kcal/mol<sup>38</sup> (from **2b** to **3b**). Clearly, Path B is energetically more favorable. The coordination of substrate to  $K^+$  ion would affect the activation of the Co–C bond of the coenzyme to initiate the catalysis.<sup>24</sup> The observed rate acceleration of the Co–C bond cleavage<sup>2h,11</sup> by the addition of substrate might originate from this coordination.

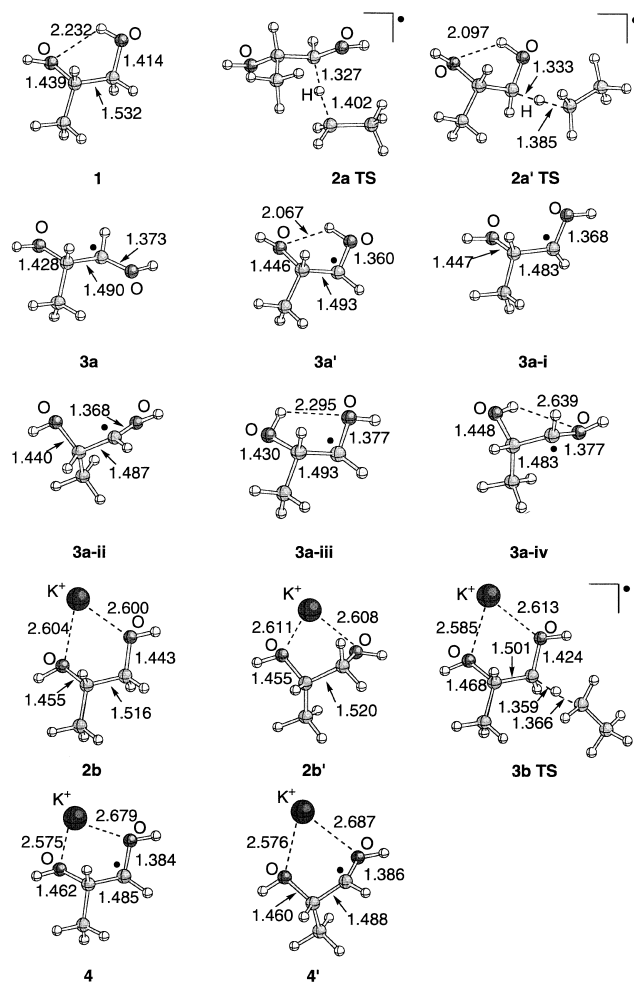
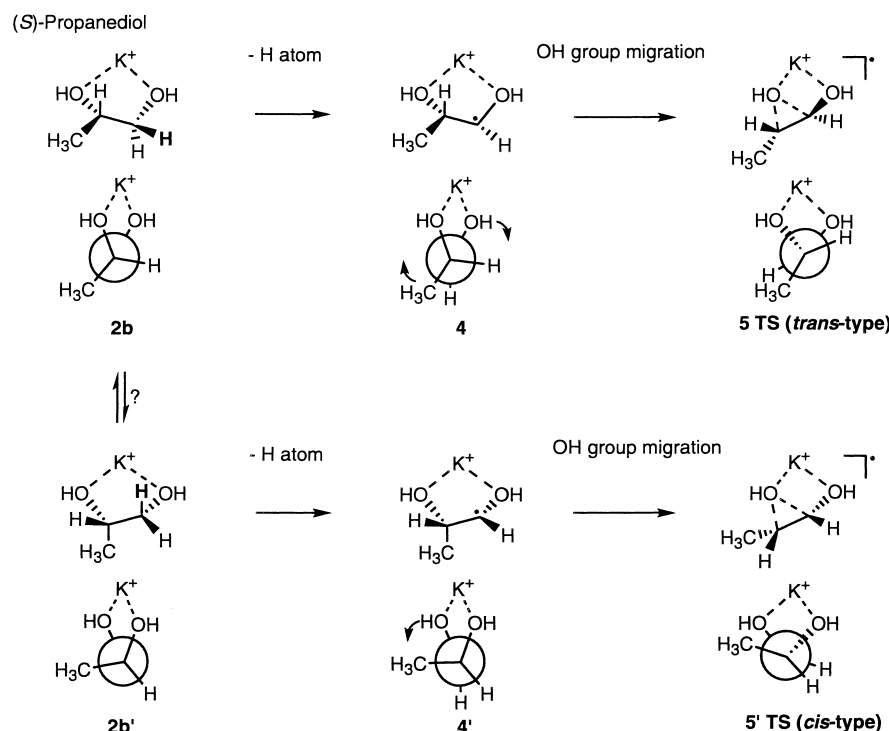


Fig. 4. Geometries in hydrogen abstraction.  $x_a$  and  $x_b$  written under each figure mean corresponding structures appearing in Path A and Path B, respectively. Bond lengths are in Å.

On the other hand, the activation energy for the hydrogen abstraction from  $C_{(2)}$  with  $K^+$  ion is 7.5 kcal/mol, and the gener-



Scheme 2.

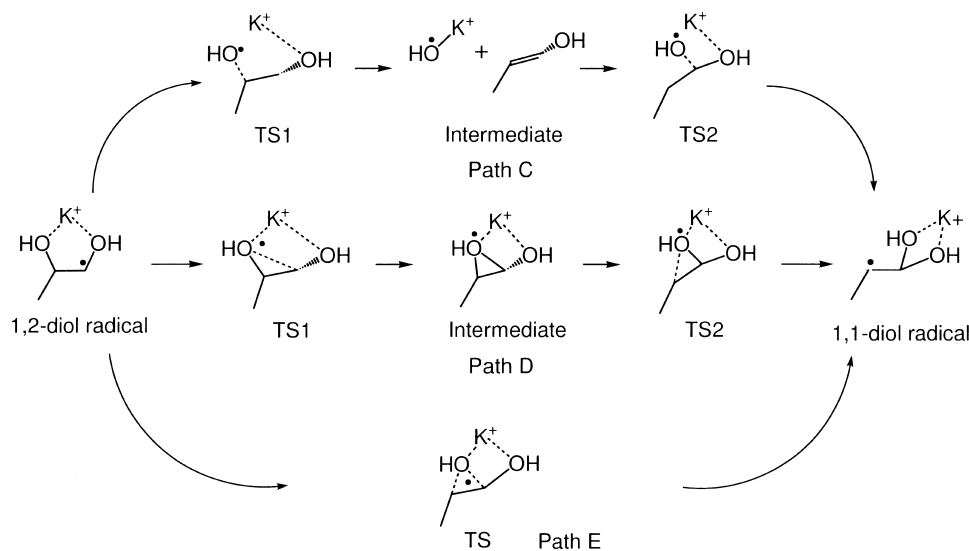
ated  $C_{(2)}$  radical species, not shown here, lies 2.4 kcal/mol below **4**, a corresponding primary radical species. Moreover, the activation energy for the other hydrogen abstraction from  $C_{(1)}$  (*pro-R* hydrogen) is near to that for the *pro-S* hydrogen abstraction (**3b**). However, the *pro-S* hydrogen atom is stereospecifically abstracted in this enzymatic process,<sup>2,10</sup> although this reaction pathway is energetically unfavorable. We therefore think that the behavior of the adenosyl group should be controlled by an environmental factor of the amino acid residues in the active site, probably the so-called adenosyl-group binding site.<sup>39</sup> Evidence for this speculation has recently been presented on the basis of the crystal structure analysis of the diol dehydratase–adeninylpentylcobalamin complex, which revealed that the C-5 atom of AdoCH<sub>2</sub> radical comes closest to the *pro-S* hydrogen on  $C_{(1)}$  of (*S*)-1,2-propanediol by rotation of the ribose moiety around the glycosidic linkage.<sup>18b</sup> Such a radical species can be viewed as a protein-bound radical rather than a free radical.

The most notable geometric feature in **2b** is the dihedral angle of  $O_{(1)}-C_{(1)}-C_{(2)}-O_{(2)}$ . Because of the steric repulsion between  $O_{(1)}$  and  $O_{(2)}$ , these four atoms and  $K^+$  ion cannot form a plane. It is noteworthy that **2b** is a local minimum structure, but it is not exactly the most stable structure on the potential energy surface. The interconversion of **2b** to **2b'** is likely to occur, as indicated in Scheme 2. The activation energy from **2b** to **2b'** is only 4.1 kcal/mol, and as opposed to our expectation, **2b'** is 1.5 kcal/mol more stable than **2b**. However, we chose **2b** to illustrate the energetics of Path B because it is the conformation actually seen in the crystal structure.<sup>18</sup> The interactions of the substrate hydroxy groups with active site residues and methyl group with surrounding amino acid residues would determine the conformation of the enzyme-bound substrate. In (*S*)-isomer, the position of the equilibrium for this in-

terconversion is considered to move over to **2b**, due to the protein surroundings.<sup>40</sup> Inhibitors that possess two or more hetero atoms having a lone pair<sup>2c,15</sup> for interaction should also be first bound to  $K^+$  ion as substrate.<sup>11</sup> A calculated net energy released upon displacement of  $(H_2O)_2$  by substrate is  $-4.9$  kcal/mol. The sum of this and the four hydrogen bond energies is the substrate binding energy which would be utilized for substrate binding (5.8–6.3 kcal/mol at 37 °C)<sup>8,14a</sup> and in part for the Co–C bond homolysis through the conformational change of protein.

In structure **4** compared with **2b**, slight changes in bond lengths of  $O_{(1)}-C_{(1)}$  (decrease by 0.06 Å) and  $K-O_{(1)}$  (increase by 0.08 Å) were observed. These derive from a slight contribution of a resonance structure possessing O-centered radical and concomitant  $C_{(1)}-O_{(1)}$  double bond because the spin density is almost localized on  $C_{(1)}$  (0.90) and a little distributed on  $O_{(1)}$  (0.10). Atom  $O_{(1)}$  becomes electron deficient in **4**, which causes an increase in the  $K-O_{(1)}$  bond. A similar tendency is seen between **2b'** and corresponding radical species **4'**, and between **2b** and the  $C_{(2)}$  radical species mentioned above. Although the  $K-O$  bond lengths in the crystal structure are 2.38 Å ( $K-O_{(1)}$ ) and 2.40 Å ( $K-O_{(2)}$ ), they are about 2.60 Å and 2.61 Å in the computed structures **2b** and **2b'**, respectively. Almost all the  $K-O$  bond lengths in each step are about 2.6 Å in our model except those in the TS structure of the OH group migration. Therefore O atoms of the enzyme-bound substrate may be a little more negatively charged by interactions with Glu<sub>170</sub> and Asp<sub>335</sub>.<sup>18a</sup>

**2. OH Group Migration:** Our previous paper<sup>24</sup> shows a possible electrostatic effect of  $K^+$  ion in this process. Taking the crystal structure<sup>18</sup> into account, let us reconsider it in more detail. Three kinds of OH group migrations were considered, as indicated in Scheme 3. The first is a stepwise fragmenta-



Scheme 3.

tion/recombination reaction that can proceed via an OH group fragmentation to form  $K^+$ -OH radical and hydroxypropene ( $HOCH=CHCH_3$ ) (Path C). The second is a stepwise abstraction/recombination reaction which is initiated by an intramolecular addition of  $C_{(1)}$  to  $O_{(2)}$  to form a stable intermediate with a three-membered ring, and then this ring is opened to give the rearranged product. The third is a concerted OH group migration (Path E). The difference between Path D and Path E is whether the three-membered ring species is a transition state or a stable intermediate. These reaction pathways are not clearly distinguished when the intermediates in Path D are energetically a little more stable than the relevant transition states, because the reaction species involved in the pathways are close in geometry.

We found that the intermediate in Path C is 21.8 kcal/mol less stable than the transition state **5** in Path E (vide infra) and that another intermediate in Path C that consists of dissociated fragments,  $K^+$ -hydroxypropene complex and OH radical, is also 22.4 kcal/mol less stable.<sup>41</sup> This fragmentation/recombination reaction are unrealistic in that the substrate cannot freely move in the cavity of the active site of the enzyme. Therefore we calculated the  $HO-K^+$ -hydroxypropene complex in which  $K^+$  ion retains the coordination interactions with the OH radical species and hydroxypropene, although these two species are entirely partitioned. However, the additional coordination leads to only 10.6 kcal/mol stabilization; thus, this complex lies 11.2 kcal/mol above the transition state in Path E. The second path (Path D) is identical to the addition/elimination mechanism reported in Ref. 42. Despite our best efforts, we could not find a transition state nor an intermediate that has a reasonable structure in Path D and could locate the transition state in Path E. For these reasons, Path E should be the most favorable pathway for the OH group migration.

In Path E the energy of substrate radical **4**, a reactant in this process, is almost identical to that of **4'**. Two and four types of transition state structures in model systems with and without  $K^+$  ion, respectively, were calculated, as shown in Fig. 5. The intramolecular hydrogen bond stabilizes reactant 1,2-dihy-

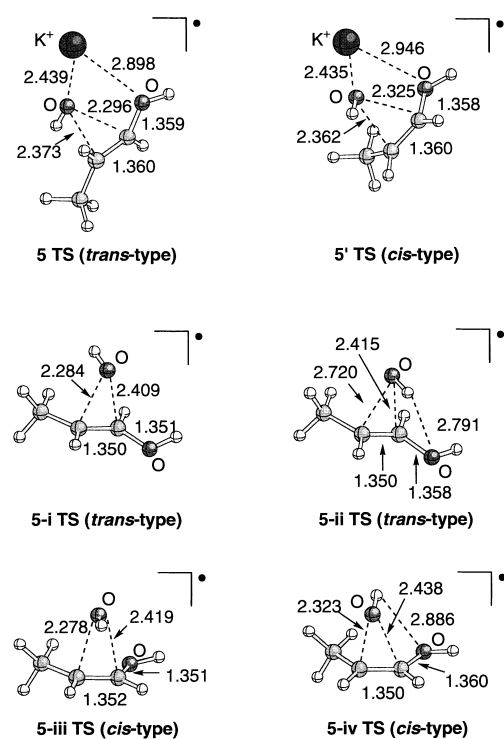


Fig. 5. Geometries of the transition states (TS) in the OH group migration. Figures in top are TSs in Path E, and in middle and bottom are TSs of the models in the absence of  $K^+$  ion. Bond lengths are in Å.

droxypropyl radical by 4.0 kcal/mol in the models without  $K^+$  ion. We do not need to consider such a hydrogen bond in the presence of  $K^+$  ion, due to the repulsion between  $K^+$  ion and hydrogen and the unfavorable H-O-C angular distortion. We see that the  $C_{(1)}-C_{(2)}$  bond lengths in these transition state structures are about 1.36 Å and 1.35 Å (close to a length of C=C double bond) in models with and without  $K^+$  ion, respectively.

Computed activation energies for this electronic process are listed in Table 1. From the structures of the reactants and tran-

Table 1. Activation Energies (kcal/mol) for Path E

A: Models with K <sup>+</sup> ion		
	TS <b>5</b>	TS <b>5'</b>
Reactant <b>4</b>	18.7	unfavorable
Reactant <b>4'</b>	unfavorable	18.3

B: Models without K <sup>+</sup> ion			
<b>3a-i</b> → <b>5-i</b>	<b>3a-ii</b> → <b>5-iii</b>	<b>3a-iii</b> → <b>5-ii</b>	<b>3a-iv</b> → <b>5-iv</b>
21.6	19.1	21.3	20.9

sition states, we conclude that **4** and **4'** should be linked with **5** (*trans*-type TS) and **5'** (*cis*-type TS), respectively, as indicated in Scheme 2. When electrostatic effects of K<sup>+</sup> ion are taken into account, the corresponding paths without K<sup>+</sup> ion are **5-i** (*trans*-type TS) and **5-iii** (*cis*-type TS) linked with **3a-i** and **3a-ii** (less stable than **3a-i** by 1.5 kcal/mol), respectively, which do not have intramolecular hydrogen bonds. As a result, decreases of activation energy through the participation of K<sup>+</sup> ion are 2.9 kcal/mol (*trans*-type TS) and 0.8 kcal/mol (*cis*-type TS). Such small effects of K<sup>+</sup> ion would not play an important role in the catalysis because the charge of K<sup>+</sup> ion can be offset by the electric field provided by amino acid residues opposite to substrate.

The reaction paths from **4** to **5** and from **4'** to **5'** are energetically almost equal in the presence of K<sup>+</sup> ion, the activation energies being 18.7 kcal/mol and 18.3 kcal/mol, respectively. His<sub>143</sub>, which has hydrogen bonding to O<sub>(2)</sub> in the crystal structure,<sup>18</sup> is important for the catalysis;<sup>43</sup> however, **5'** is not feasible for such a hydrogen bond because of the steric hindrance of the methyl group. This led us to choose the former model.

In the absence of K<sup>+</sup> ion, energetically more stable isomers of **3a-i** and **3a-ii** are formed with an intramolecular hydrogen bond, **3a-iv** lying 0.2 kcal/mol above **3a-iii**. The structures of **3a-iii** and **3a-iv** that directly link with **5-ii** (*trans*-type) and **5-iv** (*cis*-type), respectively, are shown in Fig. 4. No transition state for the OH group migration from **3a'** is found because a direct H-atom abstraction from O<sub>(1)</sub> by the OH group is energetically more favorable. The reactants used in comparing the energetics with models including K<sup>+</sup> ion are neither **3a**, **3a-i**, nor **3a-ii**, but more stable **3a-iii** and **3a-iv**. Although the electrostatic effect of K<sup>+</sup> ion is all but unavailable, K<sup>+</sup> ion can prevent intramolecular hydrogen bonding. The barrier height of 20.9 kcal/mol in the absence of K<sup>+</sup> ion (from **3a-iv** to **5-iv**) is decreased by 2.2 kcal/mol to 18.7 kcal/mol in the presence of K<sup>+</sup> ion (from **4** to **5**). We conclude in consequence that K<sup>+</sup> ion is effective for the migration and works as a hydrogen bond inhibitor of reactant radical in this process. Such a reactant destabilization is also seen in the partial proton transfer concept,<sup>21</sup> where C<sub>(2)</sub>–O<sub>(2)</sub> bond lengthening (activation) of reactant radical is caused by partial protonation in this process.

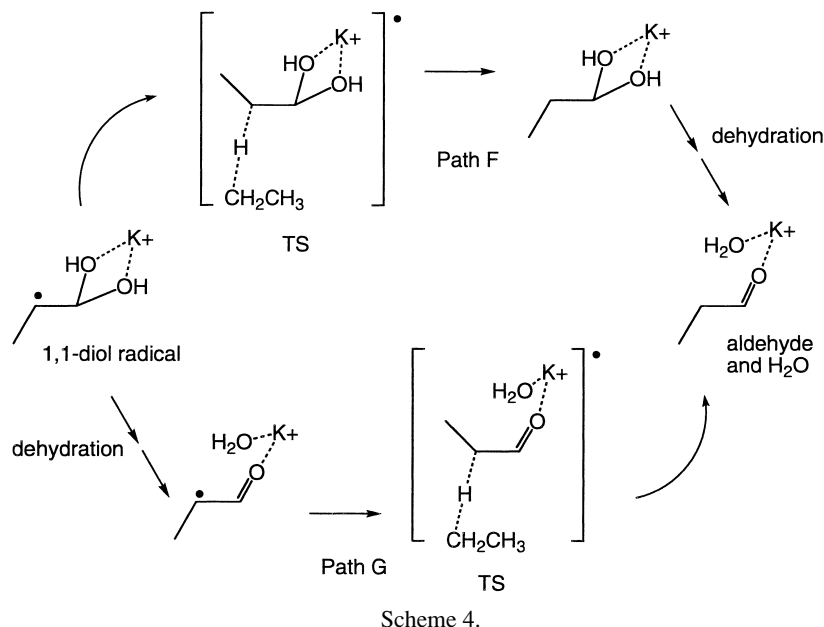
In generated 2,2-dihydroxy-1-methylethyl radical **6**, the rotation with respect to the C<sub>(1)</sub>–O<sub>(2)</sub> bond does not occur because its methyl group is held by protein or the rotation requires a high barrier.<sup>1g,44</sup> This can lead to the inversion at C<sub>(2)</sub> in the next process.<sup>10b,12</sup> However, the rotation should be permitted in ethanediol that is sterically less demanding.<sup>5</sup> Therefore racemization at C<sub>(2)</sub> of acetaldehyde (product from ethanediol) is accomplished.<sup>1g</sup>

Several mechanisms have been suggested with respect to the OH group migration or the dehydration process.<sup>1j,18,21–26</sup> The partial proton transfer<sup>21</sup> is a reasonable explanation for the decrease in activation energy for the OH group migration. Although the rate of diol dehydratase reaction is constant in a pH range from 6.0 to 10.0,<sup>13a</sup> the protonation of His<sub>143</sub> imidazole group might be possible in the transition state, irrespective of its pK<sub>a</sub> (6.0). In test calculations at the B3LYP/3-21G level of theory using a model including K<sup>+</sup> ion, 1,2-propanediol, and imidazolium ion (protonated imidazole), the computed activation energy for the OH group migration is 19.8 kcal/mol, this value being almost equal to the one for the model without imidazolium ion.<sup>45</sup> This suggests that, if the Lewis acidity of K<sup>+</sup> ion is effective even in the protein, the hydrogen bonding between substrate and His<sub>143</sub> does not have a remarkable effect on the activation energy of this process. Probably this hydrogen bond found in the crystal structure<sup>18</sup> is the one between imidazole/imidazolium proton and O<sub>(2)</sub> in the substrate, but not the one between the hydrogen on O<sub>(2)</sub> and the nitrogen in the imidazole group. If the latter is the case, such a hydrogen bond will not affect the activation energy because the hydrogen bond from imidazole to the hydrogen on O<sub>(2)</sub> makes the basicity of O<sub>(2)</sub> larger.

The activation energy from **4** to **5** (18.7 kcal/mol) is larger than that of the hydrogen abstraction from **2b** to **3b** (9.0 kcal/mol). This result is inconsistent with the conclusion from the experimental results on kinetic isotope effect that hydrogen abstraction is a rate limiting step:  $k_H/k_D = 10\text{--}13$  (overall reaction)<sup>8,10</sup> and  $k_{cat}/k_T = 20$  (overall reaction/tritium abstraction).<sup>9</sup> However, our model does not include the active-site amino acid residues. The activation energy for the OH group migration might be further decreased if the contributions of the active site residues to the TS stabilization are taken into consideration.<sup>46</sup> In the protein environment, the Lewis acidity of K<sup>+</sup> ion may be decreased by the electric field which is provided by amino acid residues coordinating to K<sup>+</sup> ion. If the Lewis acidity of K<sup>+</sup> ion in the active site is very small, the imidazolium group of His<sub>143</sub> would become much effective for lowering the activation energy for the OH group migration. In this context, theoretical calculations with more realistic models are required to examine this possibility. Very recently, Radom and co-workers proposed that the barrier height for the OH group migration is lowered by a push–pull mechanism through partial protonation/partial deprotonation.<sup>23</sup> From these considerations, the results of our calculations would not be inconsistent with the finding that the hydrogen abstraction is the rate-determining step for the overall reaction.

From the importance of His<sub>143</sub> for the catalysis,<sup>43</sup> we concluded that this residue serves as an anchor to fix the substrate in the proper position during the OH group migration and probably in the preceding and the following processes as well. In addition, this residue is likely to play an important role in the dehydration of the 1,1-diol intermediate.

**3. Aldehyde Production:** In the predissociation mechanism,<sup>25</sup> the O-atom of the product water always originates from O<sub>(2)</sub> in substrate 1,2-propanediol. However, this is inconsistent with the observed stereochemical course of the enzymatic reaction. A <sup>18</sup>O-labeling experiment<sup>4</sup> showed that the O-atom of the product water comes from O<sub>(1)</sub> when (*R*)-1,2 pro-



panediol is used as substrate, but does not come from  $O_{(1)}$  when (*S*)-1,2-propanediol is used. In addition to the reason described above for the predissociation mechanism, there is one more arguable point in the carboxylic acid cofactor mechanism<sup>26</sup> for the diol dehydratase reaction. The crystal structure analysis<sup>18a</sup> showed that carboxylic acid-containing residues which could work as a possible cofactor in this mechanism are Asp<sub>335</sub> ( $pK_a = 3.9$ ) and Glu<sub>170</sub> ( $pK_a = 4.3$ ). Because these residues are located in the rather polar environment of the enzyme and should therefore exist in the deprotonated form ( $RCOO^-$ ) under assay conditions, neither of them could serve as an essential cofactor in this mechanism.

The evidence that the dehydration reaction is not a spontaneous reaction but a catalytically controlled stereospecific one was given by the  $^{18}O$ -labeling experiment mentioned above.<sup>4</sup> It was also reported that the unhydrated aldehyde is released from the enzyme.<sup>47</sup> According to these results, the third process is also considered to proceed with the 1,1-diol intermediate that is bound to  $K^+$  ion. Two kinds of paths were considered for this process, as indicated in Scheme 4. In Path F, the recombination with a hydrogen atom from  $AdoCH_3$  is followed by dehydration from parent 1,1-propanediol. In Path G, dehydration from parent 2,2-dihydroxy-1-methylethyl radical is followed by hydrogen recombination. His<sub>143</sub> and/or Glu<sub>170</sub> can play an important role in the reaction.<sup>43</sup> Unfortunately we do not know the detailed mechanism of dehydration from 1,1-diol or its radical as yet. Glu<sub>170</sub> and/or His<sub>143</sub> are likely to work as proton carrier(s). The equilibrium between a 1,1-diol and the corresponding aldehyde in solution is well-known, and the activation energy for dehydration is quite small especially in the presence of acid or base catalyst. Similarly in diol dehydratase, the amino acid residues of which can serve as such catalysts, there would be no step in dehydration that requires a high activation energy.

An energy diagram of this process and the optimized structures for the relevant reaction species are presented in Figs. 3 and 6, respectively. In Path F, the hydrogen recombination

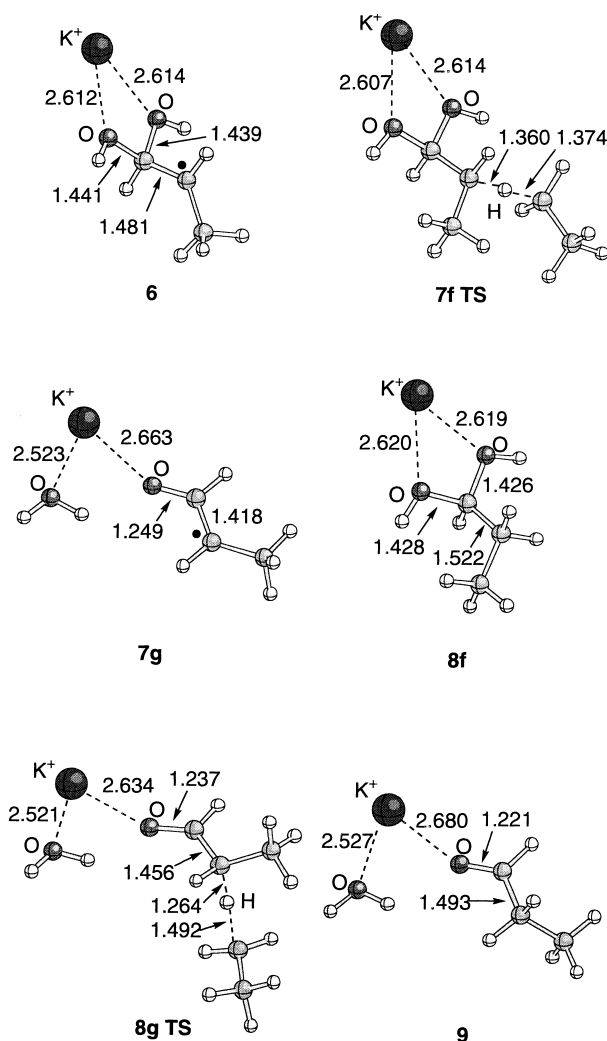


Fig. 6. Geometries in aldehyde production.  $x_f$  and  $x_g$  written under each figure mean corresponding structures appearing in Path F and Path G, respectively. Bond lengths are in Å.



from **6** to **8f** requires 15.1 kcal/mol as activation energy with a net inversion of configuration at C<sub>(2)</sub>.<sup>10b,12</sup> By the following dehydration, the energy of the system decreases by 7.3 kcal/mol when the reacting system moves from **8f** to **9**. On the other hand, in Path G stabilization of 19.5 kcal/mol is brought about by dehydration from **6** to **7g**, and the activation energy for the subsequent hydrogen recombination from **7g** to **9** is 19.8 kcal/mol. AdoCH<sub>2</sub> radical which has been formed by giving a hydrogen atom back to product radical **6** or **7g** immediately returns to Co<sup>II</sup> in cobalamin and then AdoCbl is reformed. Release of the energy upon reformation of the Co–C bond would ensure a conformational change of the protein to the substrate-free form and subsequent displacement of the product aldehyde by water, which requires an energy of 6.2 kcal/mol (from **9** to **10**<sup>48</sup>) in both Path F and Path G. The conformation of the enzyme thus returns to the initial state with two H<sub>2</sub>O molecules bound to K<sup>+</sup> ion. When the next substrate comes into the active site, it could replace the K<sup>+</sup>-bound (H<sub>2</sub>O)<sub>2</sub>. From the energetic viewpoint, Path F seems more favorable because the hydrogen recombination in Path G requires more energy than that in Path F by 4.7 kcal/mol. Stabilization upon dehydration from 1,1-diol radical in Path G leads to a marked increase in activation energy for hydrogen recombination, and the barrier would be too high if the energy released upon dehydration is not conserved in the system. For stereoselective hydrogen recombination of C<sub>(2)</sub>-centered radical, orientation of the product-derived radical must undergo strict steric control. Path F would be more likely for this reason as well because the 1,1-diol radical can be tightly bound to K<sup>+</sup> and active-site residues than the aldehyde radical.

Figures 7 and 8 show optimized geometries in aldehyde production and energy diagrams of the models without K<sup>+</sup> ion from 1,2-propanediol to propionaldehyde, respectively. The general profile of the energies in the reaction mechanism with and without K<sup>+</sup> ion is similar except for the substrate binding and the OH group migration. The most important role of K<sup>+</sup> ion in the diol dehydratase catalysis is probably to fix substrates and intermediates in proper positions to ensure the stereospecific hydrogen abstraction and the stereoselective recombination between them and the adenosyl group.

In the radical molecules formed in the previous processes, the spin density is localized on a carbon atom which is in sp<sup>2</sup>-configuration (spin density is about 0.9). We found a spin distribution in **7g**; the spin density of C<sub>(2)</sub> is 0.7 and that of O<sub>(1)</sub> is 0.3. This is reasonable in view of the well-known resonance formula indicated in Chart 2. Since such resonance structures do not contribute to **6**, the difference in activation energy originates from resonance stabilization of **7g** in Path G. The rotation of the C<sub>(1)</sub>–C<sub>(2)</sub> bond in **7g** is more strictly prohibited than that in **6**, due to the partial double bond character originating from the right resonance structure in the formula. This structural rigidity might be favorable for the inversion of configuration at C<sub>(2)</sub> in the hydrogen recombination process<sup>10b,12</sup> through Path G.

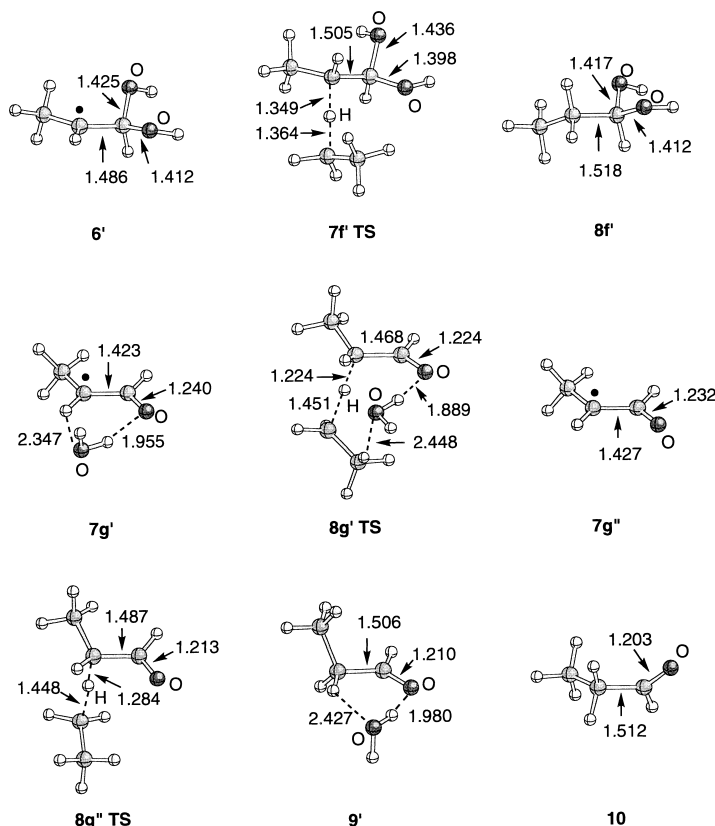


Fig. 7. Geometries of models without K<sup>+</sup> ion in aldehyde production. Bond lengths are in Å.

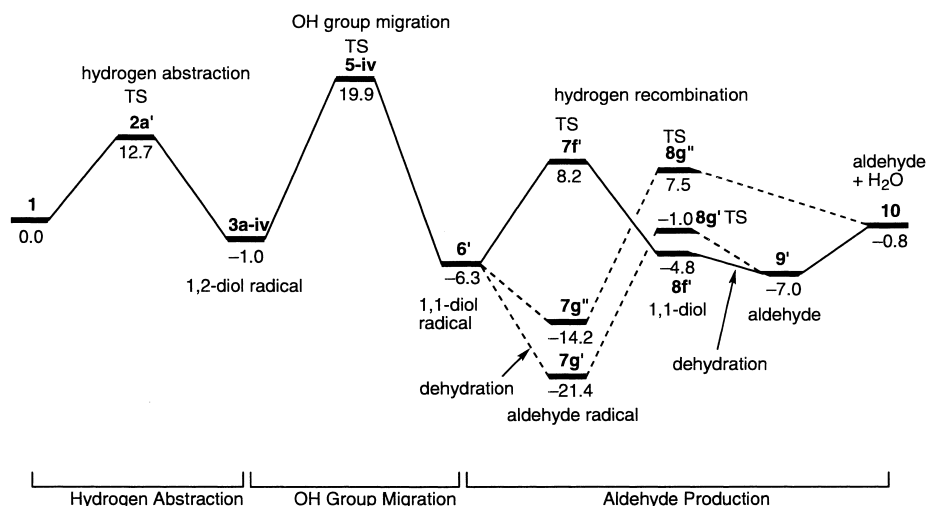


Fig. 8. Energy diagrams of the models without  $K^+$  ion along the reaction path, from 1,2-propanediol to propionaldehyde + water. In aldehyde production process:  $6'$ – $10$  (solid and dotted lines corresponds to Path F and Path G, respectively). Relative energies are in kcal/mol. Diol and aldehyde denote propanediol and propionaldehyde, respectively. On  $7g''$  and  $8g''$ ; see Ref. 51.

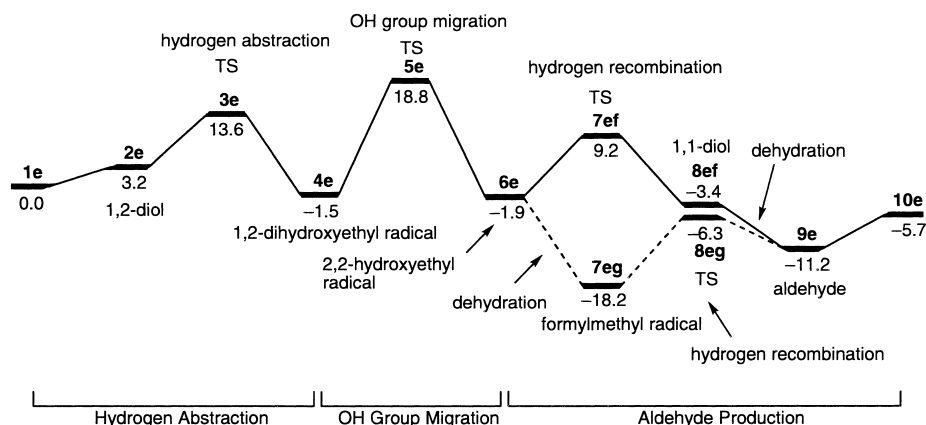


Fig. 9. Energy diagrams of the models with  $K^+$  ion along the reaction path, from 1,2-ethanediol to acetaldehyde + water. Hydrogen abstraction process:  $1e$ – $4e$  (Path B). OH group migration process:  $4e$ – $6e$  (Path E). Aldehyde production process:  $6e$ – $10e$  (Path F: solid lines and Path G: dotted lines). The path from  $9$  to  $10$  is displacement of product aldehyde from  $K^+$  ion by water. Relative energies are in kcal/mol. Diol and aldehyde denote ethanediol and acetaldehyde, respectively.

There is another path of hydrogen recombination to aldehyde radical  $7g$ . A more general one is the hydrogen recombination to oxygen-centered radical (at right in the resonance formula in Chart 2).<sup>49</sup> Generated hydroxypropene should readily tautomerize into propionaldehyde. However, such a hydrogen recombination of  $O_{(1)}$ -centered radical would rarely occur because of the steric crowding around  $O_{(1)}$  seen in the crystal structure or the distance from  $AdoCH_3$ .<sup>18</sup>

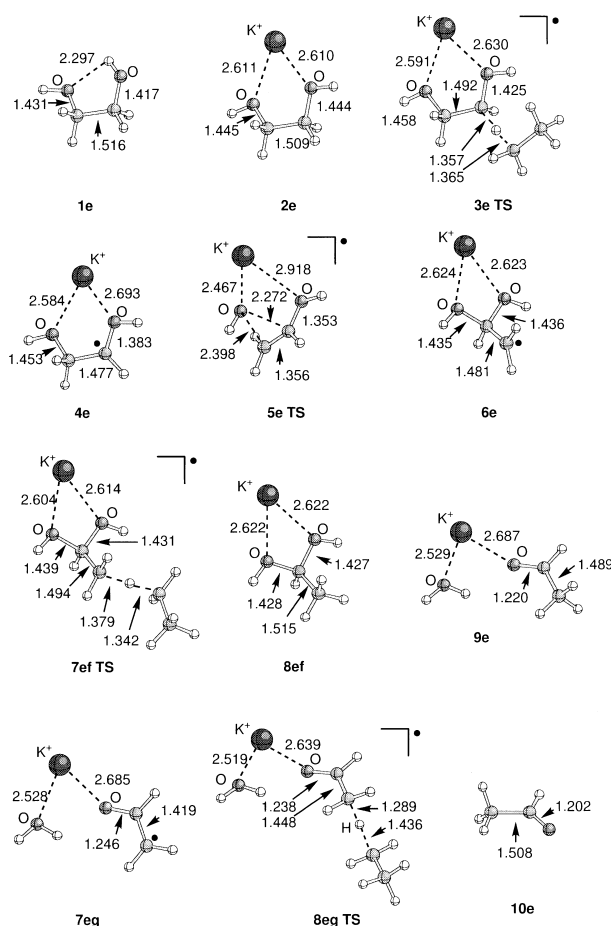
**4. Ethanediol Substrate:** On the diol dehydratase reaction as well as the 2-aminoethanol ammonia-lyase reaction, there are differences in reaction rate<sup>9,14b,15,50</sup> and KIE<sup>1c,2e,5,9</sup> between C3 and C2 substrates used. Calculations similar to those described above were carried out with ethanediol as a substrate, as shown in Fig. 9. Optimized structures for the reaction species are shown in Fig. 10. We could not find a remarkable difference in energy between propanediol and ethanediol. Although there are slight increases in activation energy of the OH group migration and hydrogen abstraction, as listed in Table 2, almost identical energies are required for

both substrates in the process of displacement of product aldehydes by water. Decreases in energy of the hydrogen recombinations in Paths F and G were calculated to be 4.0 kcal/mol and 7.9 kcal/mol, respectively. These decreases can derive from the differences of radical character in each process. That is, the primary radical reactants (2,2-dihydroxyethyl radical  $6e$  and formylmethyl radical  $7eg$ ), from the substrate ethanediol are more unstable than the secondary radical reactants (2,2-dihydroxy-1-methylethyl radical  $6$  and 1-formylethyl radical  $7g$ ) from propanediol. On the other hand, the electron spin is delocalized on both carbon atoms that can accept and supply hydrogen atoms in the transition states ( $7f$ ,  $7ef$ ,  $8g$ , and  $8eg$ ). Therefore the differences in radical character are less. This leads to activation energy lowering.

The rate of propionaldehyde formation is larger than that of acetaldehyde formation.<sup>9,14b,15</sup> The computational results suggest that the rate limiting step with both substrates should exist before the formation of 1,1-diol radical species.<sup>9</sup>

Table 2. Activation Energies (kcal/mol)

	Reactant 1,2-propanediol	Reactant 1,2-ethanediol
Hydrogen abstraction	9.0 ( <b>2b</b> to <b>3b</b> )	10.4 ( <b>2e</b> to <b>3e</b> )
OH group migration	18.7 ( <b>4</b> to <b>5</b> )	20.3 ( <b>4e</b> to <b>5e</b> )
Hydrogen recombination	15.1 ( <b>6</b> to <b>7f</b> )	11.1 ( <b>6e</b> to <b>7ef</b> )
	19.8 ( <b>7g</b> to <b>8g</b> )	11.9 ( <b>7eg</b> to <b>8eg</b> )
Displacement of aldehyde by water	6.2 ( <b>9</b> to <b>10</b> )	5.5 ( <b>9e</b> to <b>10e</b> )

Fig. 10. Geometries of models with  $K^+$  ion in the case of ethanediol. Bond lengths are in Å.

### Conclusions

We presented the entire energy profile of diol dehydratase reaction from DFT computations at the B3LYP/6-311G\* level. Based on the crystal structure, 1,2-propanediol was used as a substrate and  $K^+$  ion was taken up in the model system in which amino acid residues are excluded. In the course of the reaction, substrates and intermediates would always be kept bound to  $K^+$  ion until the release of product aldehyde from the active site. Given the neutral radical state of substrate, the OH group migration proceeds in a concerted manner. In this process  $K^+$  ion acts as an inhibitor of intramolecular hydrogen bonding, which decreases the activation energy by 4.0 kcal/mol, due to the destabilization of reactant 1,2-dihydroxypropyl radical. However, this effect of  $K^+$  ion on the activation energy for the OH migration is rather small, and thus further transi-

tion state stabilization by the protein environment must be considered to be compatible with the finding that the hydrogen abstraction is the rate determining step for the overall reaction. The neglect of the protein environment may bring about an overestimation of electrostatic effects of  $K^+$  ion because its charge would be canceled by the electric field provided by the amino acid residues near the active center. Moreover, the stereospecific hydrogen abstraction and the OH group migration need the steric hindrance of the amino acid residues and adenosyl group. The difference between the energy diagrams of the models with and without  $K^+$  ion shown in Figs. 3 and 8 is rather small except for the substrate binding and the OH group migration. We concluded that the most important role of  $K^+$  ion in the diol dehydratase catalysis is to fix substrates and intermediates in proper positions in order to ensure the stereospecific hydrogen abstraction and the stereoselective recombination between them and the adenosyl group.

The relative barrier heights for the postulated three transition states in enzymatic radical catalysis<sup>2h</sup> were obtained here for the first time with a model of the coenzyme  $B_{12}$ -dependent diol dehydratase system. These results provided theoretical evidence in support of the idea that the enzymatic radical catalysis is a mechanism of the rate acceleration by dividing a transition state with a high energy barrier into three or more transition states with lower barrier heights.<sup>2h</sup>

K. Y. is grateful for a Grant-in-Aid for Scientific Research on the Priority Area "Molecular Design and Evolution Engineering of Composite Biocatalysts" from the Ministry of Education, Science, Sports and Culture and to the Iwatani Naoji Foundation's Research Grant for their support of this work. T.T. thanks the Japan Society for the Promotion of Science for its support of this work by a Research-for-the-Future grant. Computations were in part carried out at the Computer Center of the Institute for Molecular Science.

### References

- Reviews on coenzyme  $B_{12}$ -dependent enzymes: a) B. M. Babior, *Acc. Chem. Res.*, **8**, 376 (1975). b) R. H. Abeles and D. Dolphin, *Acc. Chem. Res.*, **9**, 114 (1976). c) B. M. Babior and J. S. Krouwer, *CRC Crit. Rev. Biochem.*, **1979**, 35. d) J. Rétey and J. A. Robinson, in "Stereospecificity in Organic Chemistry and Enzymology," ed by H. F. Ebel, Verlag Chemie, Weinheim (1982), pp. 185–207. e) J. Rétey, in "Stereochemistry," ed by C. Tamm, Elsevier Biochemical Press, Amsterdam (1982), pp. 249–282. f) J. Halpern, *Science*, **227**, 869 (1985). g) J. Rétey, *Angew. Chem., Int. Ed. Engl.*, **28**, 355 (1990). h) B. T. Golding and W. Buckel, in "Comprehensive Biological Catalysis," ed by M. L. Sinnott, Academic Press, London (1997), Vol. III, pp. 239–259. i) W. Buckel

and B. T. Golding, *Chem. Soc. Rev.*, **25**, 329 (1996). j) H. Bothe, G. Bröker, U. Müller, I. Shall, S. Textor, B. T. Golding, and W. Buckel, in "Vitamin B<sub>12</sub> and B<sub>12</sub>-Proteins," ed by B. Krautler, D. Arigoni, and B. Golding, Wiley-VCH, Weinheim (1998), pp. 237–251.

2 Reviews on diol dehydratase (see also 1b,c,d,g,h): a) R. H. Abeles, in "Vitamin B<sub>12</sub>, Proc. 3rd. Eur. Symp. Vitamin B<sub>12</sub> and Intrinsic Factor," ed by B. Zagalak and W. Freidrich, W de Gruyter, Berlin (1979), pp. 373–388. b) T. Toraya, *Seikagaku*, **53**, 401 (1981) (in Japanese). c) T. Toraya and S. Fukui, in "B<sub>12</sub>," ed by D. Dolphin, Vol. 2, John Wiley & Sons, New York (1982), pp. 233–262. d) R. G. Finke, D. A. Schiraldi, and B. J. Mayer, *Coord. Chem. Rev.*, **54**, 1. (1984) e) T. Toraya, *Metal Ions Biol. Syst.*, **30**, 217 (1994). f) T. Toraya, in "Vitamin B<sub>12</sub> and B<sub>12</sub>-Proteins," ed by B. Krautler, D. Arigoni, and B. Golding, Wiley-VCH, Weinheim (1998), pp. 303–320. g) T. Toraya, in "Chemistry and Biochemistry of B<sub>12</sub>," ed by R. Banerjee, John Wiley & Sons, New York (1999), pp. 783–809. h) T. Toraya, *Cell. Mol. Life Sci.*, **57**, 106 (2000). i) T. Toraya, *J. Mol. Cat. B*, **10**, 87 (2000).

3 a) R. H. Abeles and H. A. Jr. Lee, *J. Biol. Chem.*, **236**, PC1 (1961). b) R. H. Abeles and A. M. Brownstein, *J. Biol. Chem.*, **236**, 1199 (1961).

4 J. Rétey, A. Umani-Ronchi, J. Seibl, and D. Arigoni, *Experientia*, **22**, 502 (1966). Stereochemistry of diol dehydratase and the other B<sub>12</sub> enzyme were summarized in Ref. 5, and reviewed in Ref. 1d,e.

5 D. Arigoni, in "Vitamin B<sub>12</sub>, Proc. 3rd. Eur. Symp. Vitamin B<sub>12</sub> and Intrinsic Factor," ed by B. Zagalak and W. Freidrich, W de Gruyter, Berlin (1979), pp. 389–410.

6 a) J. Stubbe, *Annu. Rev. Biochem.*, **58**, 257 (1989). b) P. A. Frey, *Chem. Rev.*, **90**, 1343 (1990). c) H. Sigel and A. Sigel Eds., *Metal Ions Biol. Syst.*, **30**, 217 (1994). d) J. Stubbe and W. A. van der Donk, *Chem. Rev.*, **98**, 705 (1998).

7 a) T. H. Finley, J. Valinsky, A. S. Mildvan, and R. H. Abeles, *J. Biol. Chem.*, **248**, 1285 (1973). b) J. E. Valinsky, R. H. Abeles, and J. A. Fee, *J. Am. Chem. Soc.*, **96**, 4709 (1974). c) K. L. Schepler, W. R. Dunham, R. H. Sands, J. A. Fee., and R. H. Abeles, *Biochim. Biophys. Acta*, **397**, 510 (1975).

8 R. G. Jr. Eagar, W. W. Bachovchin, and J. H. Richards, *Biochemistry*, **14**, 5523 (1975).

9 M. K. Essenberg, R. A. Frey, and R. H. Abeles, *J. Am. Chem. Soc.*, **93**, 1242 (1971).

10 a) P. A. Frey, G. L. Karabatsos, and R. H. Abeles, *Biochem. Biophys. Res. Commun.*, **18**, 551 (1965). b) B. Zagalak, P. A. Frey, G. L. Karabatsos, and R. H. Abeles, *J. Biol. Chem.*, **241**, 3028 (1966).

11 M. Yamanishi, S. Yamanaka, T. Omotehara, and T. Toraya, manuscript in preparation.

12 J. Rétey, A. Umani-Ronchi, and D. Arigoni, *Experientia*, **22**, 72 (1966).

13 a) H. A. Jr. Lee and R. H. Abeles, *J. Biol. Chem.*, **238**, 2367 (1963). b) T. Yamane, T. Kato, S. Shimizu, and S. Fukui, *Arch. Biochem. Biophys.*, **113**, 362 (1966).

14 a) T. Toraya and S. Fukui, *Biochim. Biophys. Acta*, **284**, 536 (1972). b) T. Toraya, T. Shirakashi, T. Kosuga, and S. Fukui, *Biochem. Biophys. Res. Commun.*, **69**, 475 (1976). c) K. W. Moore and J. H. Richards, *Biochem. Biophys. Res. Commun.*, **87**, 1052 (1979).

15 W. W. Bachovchin, R. G. Jr. Eagar, K. W. Moore, and J. H. Richards, *Biochemistry*, **16**, 1082 (1977).

16 See also Ref. 17b and references therein. For example: a)

ethanolamine deaminase: B. H. Kaplan and E. R. Stadtman, *J. Biol. Chem.*, **243**, 1787 (1968). b) glycerol dehydrase: K. L. Smiley and M. Sobolov, *Arch. Biochem. Biophys.*, **97**, 538 (1962).

17 a) T. Toraya, Y. Sugimoto, Y. Tamao, S. Shimizu, and S. Fukui, *Biochem. Biophys. Res. Commun.*, **41**, 1314 (1970). b) T. Toraya, Y. Sugimoto, Y. Tamao, S. Shimizu, and S. Fukui, *Biochemistry*, **10**, 3475 (1971).

18 a) N. Shibata, J. Masuda, T. Tobimatsu, T. Toraya, K. Suto, Y. Morimoto, and N. Yasuoka, *Structure*, **7**, 997 (1999). b) J. Masuda, N. Shibata, Y. Morimoto, T. Toraya, and N. Yasuoka, *Structure*, **8**, 775 (2000).

19 L. Salem, O. Eisenstein, N. T. Anh, H. B. Burgi, A. Devaquet, G. Segal, and A. Veillard, *Nouv. J. Chim.*, **1**, 335 (1977).

20 a) B. T. Golding and L. Radom, *J. Chem. Soc., Chem. Commun.*, **1973**, 939. b) B. T. Golding and L. Radom, *J. Am. Chem. Soc.*, **98**, 6331 (1976).

21 D. M. Smith, B. T. Golding, and L. Radom, *J. Am. Chem. Soc.*, **121**, 5700 (1999).

22 For example: a) A. L. Buley, R. O. C. Norman, and R. J. Pritchett, *J. Chem. Soc. B*, **1966**, 849. b) B. C. Gilbert, J. P. Larkin, and R. O. C. Norman, *J. Chem. Soc., Perkin Trans. II*, **1972**, 794. c) E. Hayon and M. Simic, *Acc. Chem. Res.*, **7**, 114 (1974). See also Ref. 2b and references therein.

23 D. M. Smith, B. T. Golding, and L. Radom, *J. Am. Chem. Soc.*, in press.

24 T. Toraya, K. Yoshizawa, M. Eda, and T. Yamabe, *J. Biochem.*, **126**, 650 (1999).

25 a) P. George, J. P. Glusker, and C. W. Bock, *J. Am. Chem. Soc.*, **117**, 10131 (1995). b) P. George, J. P. Glusker, and C. W. Bock, *J. Am. Chem. Soc.*, **119**, 7065 (1997).

26 P. George, P. E. M. Siegbahn, J. P. Glusker, and C. W. Bock, *J. Phys. Chem. B*, **103**, 7531 (1999).

27 J. J. Russell, H. S. Rzepa, and D. A. Widdowson, *J. Chem. Soc., Chem. Commun.*, **1983**, 625.

28 M. J. Frisch, G. W. Trucks, H. B. Schlegel, P. M. W. Gill, B. G. Johnson, M. A. Robb, J. R. Cheeseman, T. Keith, G. A. Petersson, J. A. Montgomery, K. Raghavachari, M. A. Al-Laham, V. G. Zakrzewski, J. V. Ortiz, J. B. Foresman, J. Cioslowski, B. B. Stefanov, A. Nanayakkara, M. Challacombe, C. Y. Peng, P. Y. Ayala, W. Chen, M. W. Wong, J. L. Andres, E. S. Replogle, R. Gomperts, R. L. Martin, D. J. Fox, J. S. Binkley, D. J. Defrees, J. Baker, J. J. P. Stewart, M. Head-Gordon, C. Gonzalez, and J. A. Pople, "Gaussian 94," Gaussian Inc., Pittsburgh, PA (1995).

29 a) A. D. Becke, *Phys. Rev. A*, **38**, 3098 (1988). b) A. D. Becke, *J. Chem. Phys.*, **98**, 5648 (1993).

30 C. Lee, W. Yang, and R. G. Parr, *Phys. Rev. B*, **37**, 785 (1988).

31 S. H. Vosko, L. Wilk, and M. Nusair, *Can. J. Phys.*, **58**, 1200 (1980).

32 R. Krishnan, J. S. Binkley, R. Seegar, and J. A. Pople, *J. Chem. Phys.*, **52**, 650 (1980).

33 A. J. H. Wachters, *J. Chem. Phys.*, **52**, 1033 (1970).

34 A (6211111113311111131) [8s7p2d] contraction. This is the same as a standard parameter of Gaussian 98 ab initio program for K at the 6-311G\* level of theory.

35 J. A. Cowan, in "Inorganic Biochemistry: An Introduction," 2nd ed, Wiley-VCH, New York (1997).

36 N. Shibata, Y. Morimoto, T. Toraya, and N. Yasuoka, unpublished results.

37 K<sup>+</sup>(H<sub>2</sub>O)<sub>2</sub> has a bent structure, O–K–O angle being 118.8°

The distance of K–O bonds is 2.60 Å.

38 This value lies in the typical range (7–10 kcal/mol) of hydrogen atom transfer. J. A. Kerr and A. F. Trotman-Dickenson, *Prog. React. Kinet.*, **1**, 105 (1961).

39 T. Toraya, *Arch. Biochem. Biophys.*, **242**, 470 (1985).

40 If a time from substrate binding to K<sup>+</sup> ion to hydrogen abstraction is short or binding of the hydroxy and methyl groups is strong, the equilibrium does not exist. In such a situation, there exist just two possible binding modes; an energetically favored **2b** and less favored **2b'** in the enzyme.

41 In fragmentation/recombination reaction without K<sup>+</sup> ion, the energy of intermediate (combined energy of hydroxyl radical and trans-hydroxypropene) is higher than that of TS (**5-i**) in the concerted path by 7.9 kcal/mol.

42 D. M. Smith, B. T. Golding, and L. Radom, *J. Am. Chem. Soc.*, **121**, 1037 (1999).

43 M. Kawata, N. Komoto, T. Tobimatsu, and T. Toraya, unpublished results with mutant diol dehydratases indicated that Glu<sub>170</sub> and His<sub>143</sub> are important for catalysis.

44 P. Diziol, H. Haas, J. Rétey, S. W. Graves, and B. M. Babior, *Eur. J. Biochem.*, **106**, 211 (1980).

45 Corresponding activation energy for the path from **4** to **5** at the B3LYP/3-21G level of theory is 19.8 kcal/mol. Imidazolium effect is only 1.1 kcal/mol. The reason for this less effect than Smith's model is ascribed to the participation of K<sup>+</sup> ion. In the models with K<sup>+</sup> ion, C<sub>(2)</sub>–O<sub>(2)</sub> bond in the reactant is sufficiently

elongated (activated) due to the electron withdrawing from O<sub>(2)</sub> by K<sup>+</sup> ion. When more electron rich K<sup>+</sup> ion in the enzyme was taken into account, the effect will not be so large. Therefore addition of imidazolium does not give a remarkable effect on the already electron-deficient C<sub>(2)</sub>–O<sub>(2)</sub> bond. In addition, we could not find the TS for a concerted migration at the 6-311G\* level with the model including imidazolium and K<sup>+</sup> ion.

46 Because our models exclude the amino acid residues required for the catalysis,<sup>44</sup> we cannot eliminate the possibility of activation energy lowering in the OH group migration by other mechanisms that contain partial anion radical species.

47 J. E. Valinsky and R. H. Abeles, *Arch. Biochem. Biophys.*, **166**, 608 (1975).

48 Relative energy of **10** includes propionaldehyde, K<sup>+</sup>(OH<sub>2</sub>)<sub>2</sub>, ethyl radical, and H<sub>2</sub>O. When product aldehyde is immediately hydrated after being released from K<sup>+</sup> ion or active site cavity, its energy (aldehyde that is hydrogen bonding to H<sub>2</sub>O) is –7.0 kcal/mol in Fig. 3.

49 E. S. Huyser, D. Feller, W. T. Borden, and E. R. Davidson, *J. Am. Chem. Soc.*, **104**, 2956 (1982).

50 T. J. Carty, B. M. Babior, and R. H. Abeles, *J. Biol. Chem.*, **249**, 1683 (1974).

51 On **7g''** and **8g''**, produced H<sub>2</sub>O is not hydrogen-bonding to aldehyde (separate species). See Fig. 7. Therefore those are less stable than corresponding **7g'** and **8g'**.